DE-Vol. 84-1, 1995 Design Engineering Technical Conferences
Volume 3 — Part A
ASME 1995

WAVELET ANALYSIS OF STICK-SLIP IN AN OSCILLATOR WITH DRY FRICTION

J. W. Liang
B. F. Feeny
Department of Mechanical Engineering
Michigan State University
East Lansing, MI 48824

ABSTRACT

The dynamic behavior of the transition between slipping and sticking motions of a mass-spring system with dry friction is studied numerically and experimentally. Three mathematical models of dry friction are incorporated in the forced oscillator's equation of motion. The wavelet transform is used to analyze response signals for both high and low frequency contents. For the simulated dynamical response, the wavelet transform can efficiently depict the transition characteristics in the time/frequency domain. The signatures observed in wavelet contour plot are compared to experimental results to evaluate the mathematical friction models. The wavelet transform can also be used to detect the dynamics of the sensor. The low-frequency experimental friction behavior is somewhat like the Coulomb friction model and its smooth version.

1 INTRODUCTION

Dry friction has been studied for several hundred years by researchers in control, dynamics, physics, tribology, and other communities, through graphical, numerical, analytical, and experimental methods. The work goes back to Leonardo da Vinci (1452-1519), who defined friction laws based on direct measurements. However, there is still much to understand. In this paper, we focus on stick-slip motion, which has been verified to exist in a frictional oscillator theoretically and experimentally (Den Hartog, 1930; Hundal, 1979; Shaw, 1986). Our approach is to apply the wavelet transform for analyzing the dynamical stick-slip transition behaviors. The goal is to understand the time-frequency characteristics associated with the transition from sliding to sticking in numerical and experimental acceleration signals.

If we consider a forced mass-spring with dry friction modeled by the Coulomb law, an abrupt jump in the friction force occurs at the instant that the mass sticks. On the other hand, Marui and Kato (1984) observed an oscillation in the friction force measurement when the mass stuck. The oscillation frequency may say something about the dynamics of friction. Moreover, while dealing with a boundary lubricated system, Polycarpou and Soom (1992) found similar oscillations in the acceleration signal and suggested that they were caused by the connected system's dynamical response instead of dynamical friction behavior. Nevertheless, this phenomenon deserves more attention.

In this study, we will compare simulations with experimental acceleration data. Choosing a friction model is a nontrivial task. Models range from the simple Coulomb law to complex surface descriptions. The Coulomb friction law is a great simplification, and some dynamical features of friction will not be modeled. For example, while the Coulomb friction law can model stick-slip (Shaw, 1986; Glocker and Pfeiffer, 1992) and forced response (Pierre *et al.*, 1985) in simple systems, it does not explain the hysteresis observed in sliding rocks (Ruina, 1980). Different state-variable friction models have been proposed to accommodate either hysteresis or the changing normal load case (Ruina, 1980; Dieterich, 1991; Dupont, 1994).

Three friction models will be used in our numerical study: the Coulomb law, a smooth approximation to the Coulomb law, and a state-variable law. For some range of parameters, the state-variable law used in this study, applied as a substitute for the Coulomb law, will cause some oscillation in acceleration signals during the transition from sliding to sticking. The smooth friction law is a continuously differentiable version of Coulomb friction law, and it is included to model the possibility in which no true sticking can be observed.

The wavelet transform, an alternative to the classical Fourier transform, is of interest for the analysis of transient signals. The basic difference is as follows. In contrast to the Fourier transform, which uses complex sinusoids as basis functions and averages the signal over an infinite time interval to obtain frequency information, the wavelet transform uses a "mother wavelet" together with dif-

ferent window sizes and time locations to generate its basis functions. The wavelet transform has attracted the attention of vibration researchers. For example, Newland (1994) developed discrete wavelet transform maps and analyzed some transient vibration signals. Önsay and Haddow (1994) used wavelet transform to analyze the transient wave propagation behavior of beam vibration in dispersive medium. A particular property of this transform is its ability to identify and isolate the fine temporal, high-frequency structure of a signal. The high-frequency stick-slip events associated with the low-frequency forced response suggest that a stick-slip signal is a good candidate for applying the wavelet transform.

In the longterm the wavelet transform may help in the study of stick-slip, perhaps in understanding the connection between the normal-directional motion and tangential sliding frictional behavior which was emphasized by Oden and Martins (1985). Evidence shows that the normal-directional motion has frequency contents much higher than the tangential ones, such that it might be possible to distinguish the individual effect in different directional dynamics through the use of the wavelet transform. Moreover, it is known that a controlled dither input can eliminate stick-slip (Armstrong-Hélouvry *et al.*, 1994). Through the identification of frequency contents in transition behaviors, some insight might be obtained for choosing the applied dither signals.

In the section below, a brief description of the mathematical model for single degree of freedom oscillator associated with each friction law will be given.

2 SYSTEM MODELS

The system under investigation is a base-excited mass-spring system constrained to move in one dimension in the presence of dry friction (Figure 1). The differential equation for this model is

$$m\ddot{X} + kX + \beta f = kY(t), \tag{1}$$

where βf indicates friction force, X is the displacement of the mass, and $Y(t) = Y_0 \cos \omega t$ denotes the base-excitation displacement. We neglect viscous friction, since it is small, and dry friction dominates.

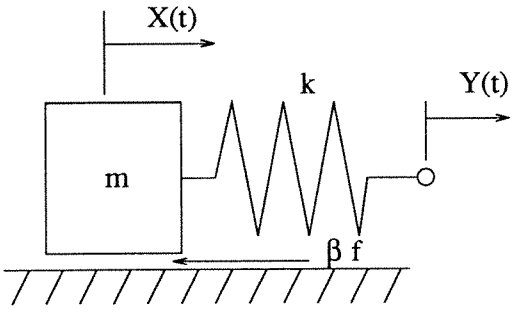

Figure 1: The forced oscillator with dry friction

In using the Coulomb law, we assume that there is a static coefficient of friction μ_s and a kinetic coefficient of friction μ_k. When the mass is at rest, the static friction will take the values necessary to balance forces. Thus, the normalized friction relation $f(\dot{X})$ is multi-valued at $\dot{X} = 0$. Assuming $\mu_s = \mu_k$ (which may be reasonable in some cases but not others), the normalized friction function $f(\dot{X})$ is given by

$$\begin{aligned} f(\dot{X}) &= 1, \quad \forall\ \dot{X} > 0; \\ -1 < f(\dot{X}) &< 1, \quad \dot{X} = 0; \\ f(\dot{X}) &= -1, \quad \forall\ \dot{X} < 0. \end{aligned} \tag{2}$$

If we let $\omega_n^2 = k/m$, $\tau = \omega_n t$, and $x = m\omega_n^2 X/\beta$, the non-dimensional equation becomes

$$\ddot{x} + x + f(\dot{x}) = a\cos(\Omega\tau), \tag{3}$$

where $a = Y_0 m\omega_n^2/\beta$, and $\Omega = \omega/\omega_n$. In equation (3) " $\dot{x}$ " refers to differentiation of x with respect to τ. The model represented by equation (3) can have stick-slip motion for a range of parameter values. This has been shown analytically by Den Hartog (1930), Shaw (1986), Hundal (1979), and Pierre *et al.* (1985), and experimentally by Marui and Kato (1984).

There are other possible candidates for friction models. A smooth approximation of Coulomb friction law can be written as

$$f(\dot{x}) = \tanh(\alpha\dot{x}), \tag{4}$$

where α is a parameter that determines the closeness between the discontinuous Coulomb model and its smooth approximation. The convenience of using a smooth friction function is that we need not be concerned with the presence of discontinuity while performing the numerical integration. Applying this model to the system in Figure 1, the non-dimensional equation of motion will be the same as equation (3), with $f(\dot{x})$ expressed as in equation (4).

State-variable friction laws, based on the observation of friction measurements, have been used to model different frictional systems successfully (e.g. Ruina, 1980; Dieterich, 1991; Feeny and Moon, 1994). In these models there exists an additional "hidden" state, which depicts the dynamic friction behavior. While this additional state plays the role of the coefficient of friction, for nonzero velocity, it evolves with time. If we apply a state-variable law to the previous system in the place of the Coulomb law, we have

$$\ddot{x} + x + \theta = a\cos(\Omega\tau) \qquad \dot{\theta} = -\gamma(\theta - f(\dot{x})) \tag{5}$$

where $f(\dot{x})$ is a Coulomb-like backbone function, θ is the state that can be thought as instantaneous value of the friction coefficient, and γ defines the rate at which θ tracks $f(\dot{x})$ asymptotically. As $\gamma \to \infty$ the system in equation (5) approaches the 1 DOF system in equation (3) because the attraction strength of the force θ to $f(\dot{x})$. In order to simplify the study, the backbone function will be taken as the smooth version of Coulomb friction law, namely, equation (4) instead of equation (2).

The following section shows a brief review of the wavelet transform analysis and its computation scheme.

3 WAVELET TRANSFORM

In contrast to Fourier transform, wavelet transform has "short" high frequency basis function and "long" low frequency ones.

Therefore, it can use the short basis functions to fetch the information contained in the events which happen during a short time interval, but will not lose the low frequency events. This zooming property of wavelet transform is achieved by translating and dilating a "mother wavelet". The mathematical definition of continuous wavelet transform is given as an inner product of a signal and a particular set of functions

$$CWT_x(a,b) = \int_{-\infty}^{\infty} x(t) h^*_{a,b}(t) dt. \qquad (6)$$

where $h^*(t)$ stands for the conjugate of $h(t)$. Equation (6) measures the "similarity" between the signal and the basis functions

$$h_{a,b}(t) = \frac{1}{\sqrt{|a|}} \; h(\frac{t-b}{a}) \qquad (7)$$

called wavelets, where $a, b \in \Re$, $a \neq 0$, and the constant $1/\sqrt{|a|}$ is used for energy normalization. The parameters a and b determine the dilation and translation of the mother wavelet, which is chosen here as the Morlet wavelet (Morlet and Arens, 1982), and is given by

$$h(t) = \pi^{-1/4}(e^{-i\omega_c t} - e^{-\omega_c^2/2}) e^{-t^2/2}, \qquad (8)$$

where ω_c is the center frequency of the mother wavelet. The second term in the bracket on the right-hand side of equation (8) exists for the purpose of the reconstructing (or inverse) process. In practice, it can be neglected (Önsay and Haddow, 1994). Therefore, it will not be included in our calculations. The mother wavelet is stretched for large values of a, thus becoming a "long" low frequency function. Similarly, it becomes a "short" high frequency function when a takes small values.

In order to implement the calculation of the wavelet transform, a sublattice is constructed by discretizing the values of a and b. By fixing the dilation and translation step size to a_0 and b_0, and defining

$$a = a_0^m; \qquad b = n b_0 a_0^m \qquad (9)$$

with $m, n \in \mathbf{Z}$, results in

$$h_{mn}(t) = a_0^{-m/2} \; h(a_0^{-m} t - n b_0). \qquad (10)$$

The translation step depends on the dilation, since long wavelets are advanced by large steps, and short ones by small steps. On this discrete grid, the wavelet transform is thus

$$WT_x(m,n) = a_0^{-m/2} \int_{-\infty}^{\infty} h^*(a_0^{-m} t - n b_0) x(t) dt. \qquad (11)$$

Of particular interest is the discretization on a dyadic grid, which occurs for $a_0 = 2$, $b_0 = 1$, and is used in this study. To implement the calculation of wavelet coefficients, $WT_x(m,n)$, the numerical integration scheme is adopted. This algorithm may not be efficient in the sense of computation. However, the number of data points in this study is not huge. When applied to benchmark signals such as sinusoids and impulses, this algorithm gave reasonable results. There are other algorithms which can be found in the signal processing literature (Önsay and Haddow 1994; Newland, 1994).

4 NUMERICAL STUDIES

This section includes numerical examples of stable stick-slip motion and their corresponding wavelet transforms. The numerical integration of the Coulomb friction model is difficult because of the discontinuity at zero velocity. Many researchers have proposed prescriptions for solving this problem (Shaw, 1986; Feeny and Moon, 1994; Meijaard, 1994). This study follows the method used in Feeny and Moon (1994). In the numerical integration scheme, conditions for sticking (or sliding) can be determined by defining the sticking region (Shaw, 1986; Feeny and Moon, 1994). There can be different stick-slip motions for this system, including none, one, two, or many stops per cycle. Detailed analyses about the motion types and their corresponding parameter space can be found in previous research results (Shaw, 1986; Hundal, 1979; Marui and Kato, 1984).

The numerical study of the Coulomb model concentrates on the parameter values $\Omega = 0.37$, and $a = 1.5$. The parameter "a" is not chosen from an experimentally measured value, but as a value which produces behavior qualitatively similar to the experiment. With our current experiment set-up, we are unable to measure the friction, and hence the force ratio "a". Nevertheless, this should not have a large effect on the study of dynamical frictional behavior.

Figure 2 shows the acceleration (and displacement) response together with the wavelet transform contour plot for the Coulomb friction case. The displacement plot depicts a stable stick-slip motion with two stops per cycle. Due to the discontinuity of the Coulomb friction model, the acceleration response has an abrupt jump at the instant that the mass sticks, and has another sharp corner when the mass starts to slide (if $\mu_s > \mu_k$, the sharp corner would instead appear as a jump). Both of these transitions involve high-frequencies to different degrees, with the jump having higher frequency content.

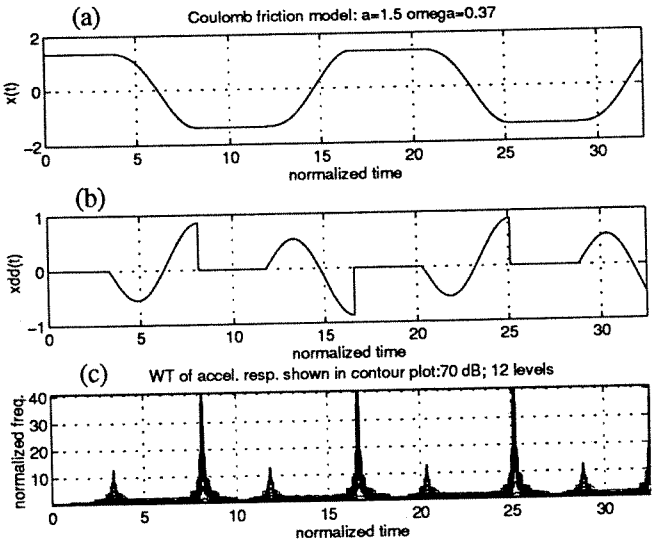

Figure 2: Numerical simulation of stick-slip motion with the Coulomb friction model: (a) displacement (b) acceleration response (c) contour plot of wavelet transform of acceleration signal

The wavelet transform is calculated in accordance with equation (8)-(11) with $\omega_c = 4$. To calculate the wavelet coefficients,

$WT_x(m,n)$, which correspond to elements on a grid in the time-frequency plane, we use numerical summation during a finite time interval equal in length to the time length of acceleration signal. At both ends of the time axis, there are some irregularities in the spectrum. Theses irregularities occur because the data values beyond those two ends are set to be zero. This distorts the spectrum when the convolution of the wavelets, $h^*(t)$, and signal, $x(t)$ is conducted. The contour plot represents the logarithmic values of the each coefficient's magnitude. The blank region in the plot contains values which are 70 dB below the maximum value. There are twelve levels spanning the 70 dB range. The wavelet transform plot exposes spikes corresponding to the jumps described above. It also has small spikes which correspond to the sharp corners associated with the onset of slip. It is reasonable that the latter spikes are smaller because no jump of the signal is involved.

A numerical simulation of the smooth Coulomb friction case is shown in Figure 3.

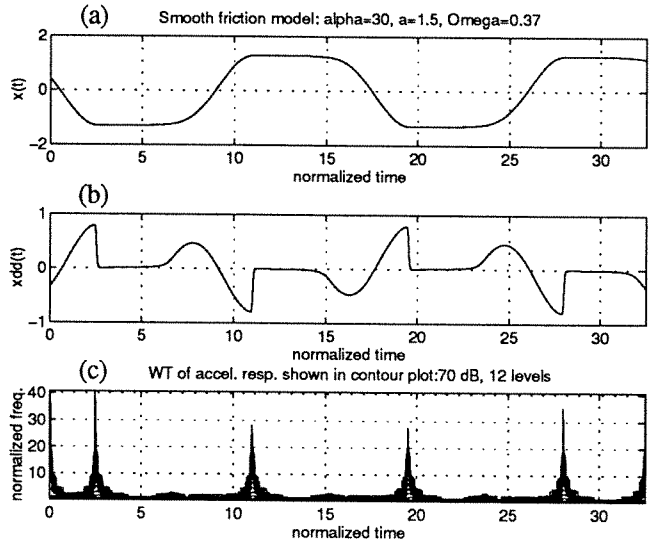

Figure 3: Numerical simulation of stick-slip motion with the smooth friction model: (a) displacement (b) acceleration response (c) contour plot of wavelet transform of acceleration signal

In this case, we used equation (3) and (4) with $a = 1.5$, $\Omega = 0.37$, and $\alpha = 30$. It is not surprising that the resulting responses look quite similar to Coulomb friction case (except that the sharp corners in acceleration signal do not appear, and no real sticking occurs), since the smooth friction model is an approximated version of the Coulomb friction. The qualitative characteristics in time domain traces are similar to the previous case. For example, there are two near stops per cycle, and there are sudden changes in the acceleration signal, although those changes are continuous. The corresponding wavelet contour plot also illustrates the same features as in Figure 2, except that the small spikes do not exist obviously. The main spikes corresponding to the transitions from sliding to sticking are also less pronounced in this case.

Next, we present numerical results with a state-variable friction model. In contrast to Figures 2 and 3, Figure 4 shows different features in transition zones. Parameter values for this simulation are $a = 1.5$, $\Omega = 0.37$, $\alpha = 50$, and $\gamma = 10$. While there are still two near stops per cycle, the mass does not "stick" immediately during the transition from sliding to sticking. The state-variable yields some oscillations in the transition between slip and "stick". Though there is no visible movement in the displacement response, the displacement is not absolutely constant when the oscillations in acceleration take place. The wavelet contour plot also illustrates different characteristics. Rather than being symmetric with respect to the spikes, the blurred low-frequency spectrum corresponds to oscillations in acceleration signal. As with the smooth friction case, there is a "smooth" transition when the mass starts to slide. Thus no lower spikes are observed.

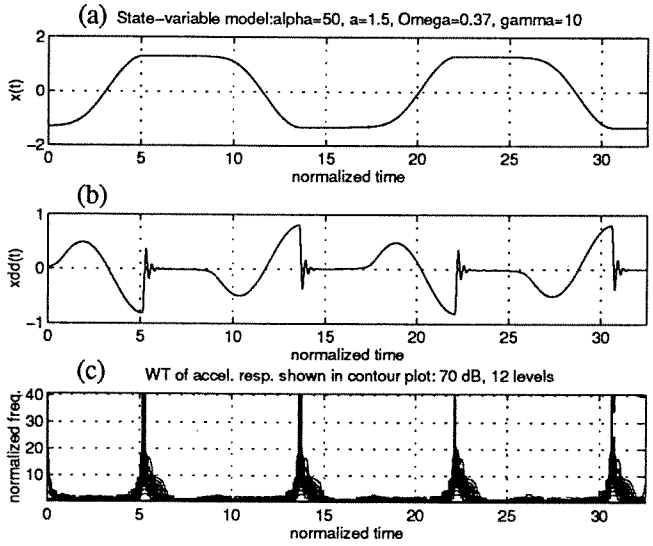

Figure 4: Numerical simulation of stick-slip motion with the state-variable friction model: (a) displacement (b) acceleration response (c) contour plot of wavelet transform of acceleration signal

According to the observations made from Figures 2, 3, & 4, different friction models have different time/frequency signatures, which are expected to help us in seeking similarities between the simulating and experimental results. The next section will describe the experiment apparatus, results of pretests of the set-up, and some experimental studies of stick-slip motion.

5 EXPERIMENTAL INVESTIGATIONS

5.1 Apparatus and Instrumentations

The experiment consists of a mass attached to a cart, three parallel-connected helical springs, an air-curtain guiding mechanism, and an electromagnetic shaker. The schematic diagram is shown in Figure 5. To sense the motion, we used the seismic accelerometer (PCB, Model 393c), which has the frequency range 0.025 to 800 Hz, and sensitivity 1 Volt/g. Most of the mass consists

of the accelerometer. The total mass is 1.83 kg.

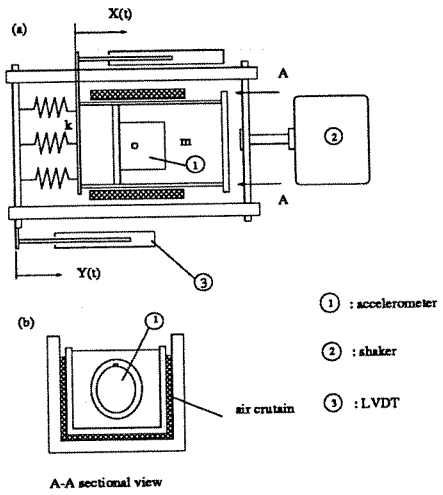

Figure 5: Experimental set-up: (a) top view (b) side view

The accelerometer signal was amplified by using standard power unit (PCB, Model 480M43). A battery-powered unit was chosen because of the low inherent noise. The accelerometer was placed on the central position of the cart, which was made of aluminum plates. In order to remove the friction, the cart was supported by a three-surface air curtain, as shown in Figure 5(b). A pressure stabilizer was used to control air pressure on each surface. In doing the frictional study, the air pressure was kept low such that the net force built up on the bottom surface could not support the weight of the cart. Hence, there was a true contact on the bottom surface. Due to the fact that the friction and exciting forces were not applied on the same line, there will be a nonuniform normal load to compensate the time-varying frictional moment. The air curtain on two sides of the cart can guide its motion in a prescribed direction with negligible friction. The counter surface which had contact with the cart was made of ground stainless steel. The aluminum surface was ground and coated. There was surface contact between the aluminum and bottom track (made of ground stainless steel).

The electromagnetic shaker (LDS, Model 400), with a power amplifier/signal generator (LDS, Model P0300), is capable of producing a harmonic signal to excite the cart. The lowest operating frequency for which the shaker can produce satisfactory harmonic signal is 1 Hz. The maximum displacement amplitude is 8 mm. During the experiment, the typical amplitude of excitation was about 3 mm. The displacement $X(t)$ of mass m, and base-excitation displacement, $Y(t)$, were measured by linear variable differential transformer (LVDT, Robinson-Halpern CO., Model 210A-1000). The data-acquisition system consists of a Macintosh computer, 12-bit A/D converter (National Instrument, Model NB-MIO-16), and data-acquisition software (LabView 3.0).

5.2 Pretest and Apparatus Dynamics

Pretest were conducted to obtain the noise level. The noise power spectrum level was 80 dB below the signal power spectrum level in the range of DC to 2500 Hz. The main system's natural frequency was 5.37 Hz, which was determined by a free vibration test with a full air curtain. Under this condition, the viscous damping ratio was 0.0032.

In order to distinguish the sensor dynamics from the dynamical friction behavior, a pretest of the accelerometer mount was executed. The system containing the accelerometer and its mounting structure will be denoted as the subsystem. The test was conducted when the cart was locked and subjected to a impulse excitation produced by a general-purpose impulse hammer (PCB, Model 086c03). This impulse-excitation test was used to understand the case in which mass sticks suddenly and there is an abrupt change of acceleration, reminiscent of a step excitation. Figure 6 illustrates the dynamical response of the subsystem. It includes the acceleration response in time domain and its corresponding wavelet contour plot.

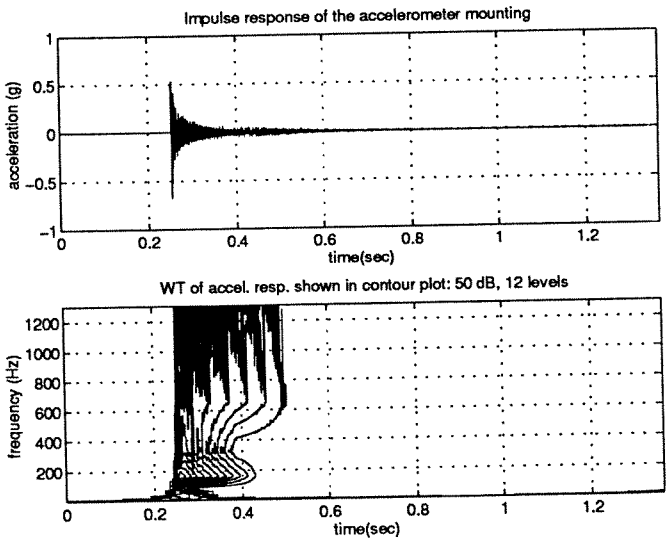

Figure 6: Acceleration signal and corresponding wavelet contour plot for an impulse-response in the accelerometer's mounting

The wavelet contour plot shows a striking tail structure corresponding to the fundamental frequency of this subsystem. According to Figure 6, the first fundamental frequency of this subsystem is close to 200 Hz, which is much higher than that of the main system. The results in Figure 6(b) were verified by comparing the frequency domain information with the results obtained by the FFT method. The characteristics in Figure 6 can also be used to determine if there is any dynamical behavior induced by this mounting, affecting the sensing of stick-slip motion.

5.3 Experimental Studies of Stick-Slip Motion

Some examples of stable stick-slip motions obtained in the experiment will be shown in this section. These results were all obtained

under the following conditions: (a) the observed motions had existed more than half of an hour; (b) there was low air pressure such that the cart had an anti-friction guide on the sides and also a bottom contact with the stainless steel surface; (c) for the wavelet transform contour plot, a 50 dB gap was set between the minimum and maximum magnitude of wavelet coefficients, with 12 level curves spanning this range to illustrate the magnitude distribution.

Figure 7 recorded a typical base-excitation displacement, $Y(t)$, which is much like a sinusoidal signal. The excitation frequency in Figure 7 is 2.5 Hz. Figure 8 includes the displacement response, $X(t)$, the acceleration response, $\ddot{X}(t)$, and its corresponding wavelet contour plot for the 3.0 Hz excitation frequency case.

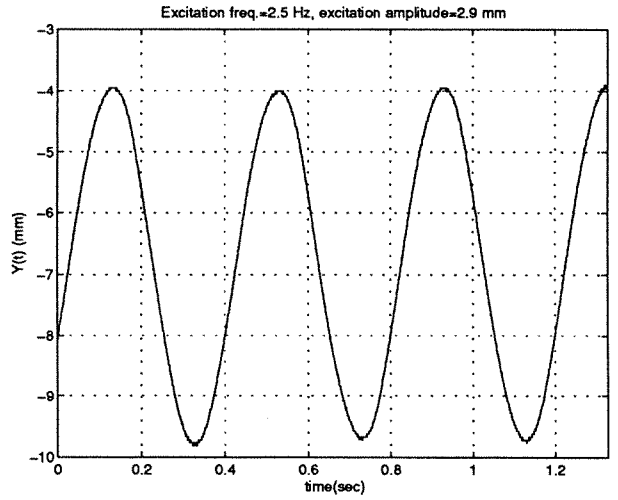

Figure 7: Experimental base excitation motion

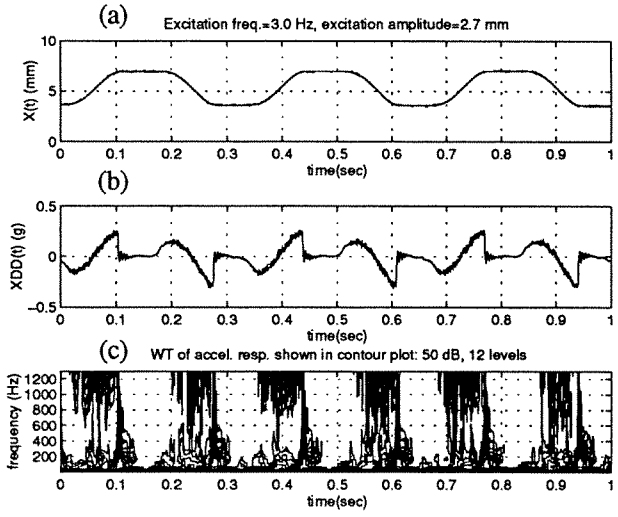

Figure 8: Experimental stick-slip motion with 3.0 Hz excitation: (a) displacement (b) acceleration time response (c) wavelet contour plot of acceleration signal

In accordance with Figure 8, some observations can be made. (1) There are two stops in each cycle. This is qualitatively similar to the simulation results. Clear definition of sticking in the real world depends on the scale of viewing. Therefore, when we say that there are two stops in each cycle, we mean that there is no visible slip motion during two time intervals per cycle, and the displacement trace indicates a constant response. (2) During the transition from sliding to sticking, some high-frequency oscillation occurred. These oscillations might lead us to think that illustrated evidence has been obtained for state-variable friction model in this system. However, this is not true! We focus on the wavelet contour plot and compare it with the pretest results on the accelerometer mounting. The dominant part of the high-frequency oscillation in Figure 8 corresponds to the fundamental natural response of the accelerometer mounting. A similar observation has been obtained by Polycarpou and Soom (1992), in which the boundary-lubricated transition from sliding to sticking was investigated. This observation shows that the wavelet transform can efficiently detect different effects involved in a dynamical response. On the other hand, the real dynamical friction features may be covered by the subsystem's response. An idea for handling this problem, in the signal processing point of view, might be the addition of a low-pass filter to remove the accelerometer dynamics. Nevertheless, due to the step-like nature of the acceleration jumps, Gibbs phenomenon will occur and cause other low-frequency oscillations to show up if the filter were applied. (3) The phenomenon observed in (2) can be explained by the fact that there exists an abrupt jump in acceleration response, which can be interpreted as a step effect in the subsystem. Therefore, the subsystem's dynamical response is excited. The extent to which these dynamics are involved will depend on the magnitude of the acceleration jump, which will be verified in the later cases with lower excitation frequency. (4) During the sliding phase, random fluctuations of the acceleration signal occurred. This phenomenon may have something to do with the normal contact vibration or surface roughness. (5) A remarkably "smooth" acceleration signal was shown at each onset of sliding, and its occurrence seems to be independent of the excitation frequency or the magnitude of the acceleration jump. Since it happens during a significant time interval with invisible displacement change, it inspires us to speculate about microsliding or normal vibrations.

Similar to Figure 8, Figures 9 and 10 illustrate cases in which the excitation frequencies are 2.0 Hz and 1.5 Hz. The 2.0 Hz case corresponds to the simulation case in the sense that the normalized frequency, Ω, is approximately equal to this excitation frequency divided by the main system's natural frequency. According to the observations made with respect to Figure 8, different features are given from Figure 9, & 10 and described as the following. (1) Although similar subsystem dynamics can still be observed in Figures 9 and 10, it becomes weaker. This is evident by looking at acceleration time traces or wavelet contour plots. It is possibly caused by smaller acceleration changes or a smoother transition. (2) If we concentrate more in the acceleration time trace (especially, in Figure 9), a low-frequency, small-amplitude oscillation can be observed right after the transition instant from sliding to sticking. This gives us hope to further investigate the existence of dynamical friction behavior, if the subsystem dynamics can be excluded and the noise level can be lowered. However, the resolution of wavelet contour plot needs to

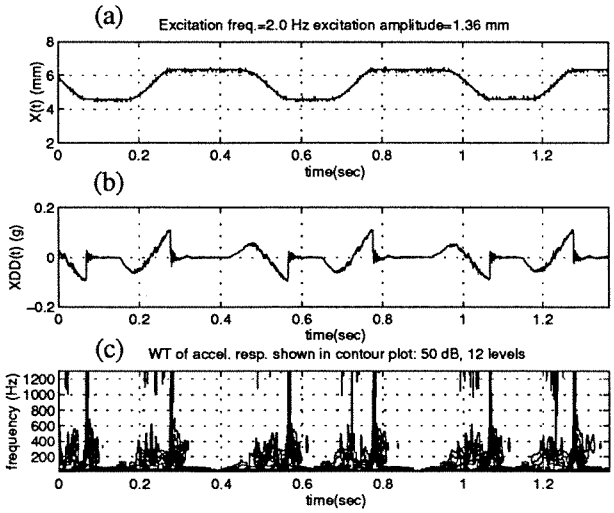

Figure 9: Experimental stick-slip motion with 2.0 Hz excitation: (a) displacement (b) acceleration time response (c) wavelet contour plot of acceleration signal

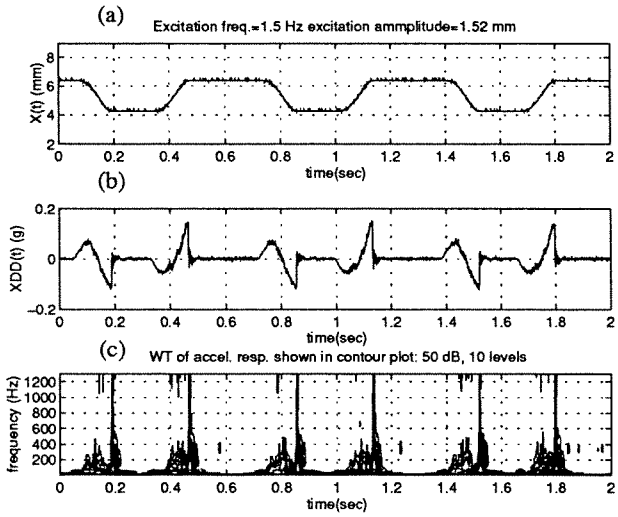

Figure 10: Experimental stick-slip motion with 1.5 Hz excitation: (a) displacement (b) acceleration time response (c) wavelet contour plot of acceleration signal

be increased to magnify the effect of such a small-amplitude oscillation. (3) Longer sticking times existed for these cases, during which there was a noisy acceleration signal in the case of 1.5 Hz excitation. This is suspected to have something to do with the shaker dynamics, microslip, or normal vibrations.

In order to further compare the experimental results with different simulation results, we zoom in on the low-frequency range of the wavelet transform plot. Figure 11(a), (b), and (c) show the simulated acceleration responses of Coulomb, state-variable, and smooth friction models. These plots are the same as in Figure 2, 3, and 4 except for the frequency range of the wavelet transform plot. Figure 11(d) shows the experimental acceleration response corresponding to the 2.0 Hz excitation frequency. The range of the frequency in both simulation and experimental results are nearly equivalent if one converts the experimental data into normalized time coordinate. Furthermore, since the experimental data contains noise, the wavelet transform plot in Figure 11(d) was shown in different dB range for a clearer presentation.

By observing structures in different wavelet transform plots of Figure 11, some qualitative observations can help in validating the friction model. For example, although the Coulomb model cannot describe all the features in the experimental results, it does predict the abrupt jump at the onset of sticking. For the transition from stick to slip, the smooth and state-variable friction models seem to work better in the sense that they depict a less pronounced spike in the wavelet transform plot.

6 DISCUSSIONS AND CONCLUSIONS

This study shows that the wavelet transform can be used to distinguish different simulation friction models by obvious features shown in the time-frequency plane. This is helpful in investigating a complicated dynamical behavior such as the transition of stick-slip motion. From the lower-order dynamical system point of view, the Coulomb friction model or its smooth version may be enough to describe the frictional oscillator like the one in this study. The existence of "hidden" state in the transition zone is rather a open question, since some acceleration time traces did show a small-amplitude oscillation.

There are some aspects of the experiment set-up which can be enhanced for future work. For example, different combinations of materials may have different features in frictional study, which can be included. We believe that ground surfaces are more general compared with the polished ones in an industrial sense. However, it is worthwhile to try surfaces with various properties. For applying the wavelet analysis, including the phase of the wavelet transform might help in interpreting the time/frequency domain information. The environmental dynamics can dominate if its frequency response cannot be separated from that of the frictional main system. For instance, the coupling between the dynamics of the main system and subsystem in this study is strong enough that the dynamic friction behavior might be concealed by the subsystem's response. Increasing the stiffness of the mount of the measuring device will help isolate its dynamics from the main system. The friction force and normal load should be measured in order to estimate the normalized parameters of experimental system, so that a more quantitative comparison can

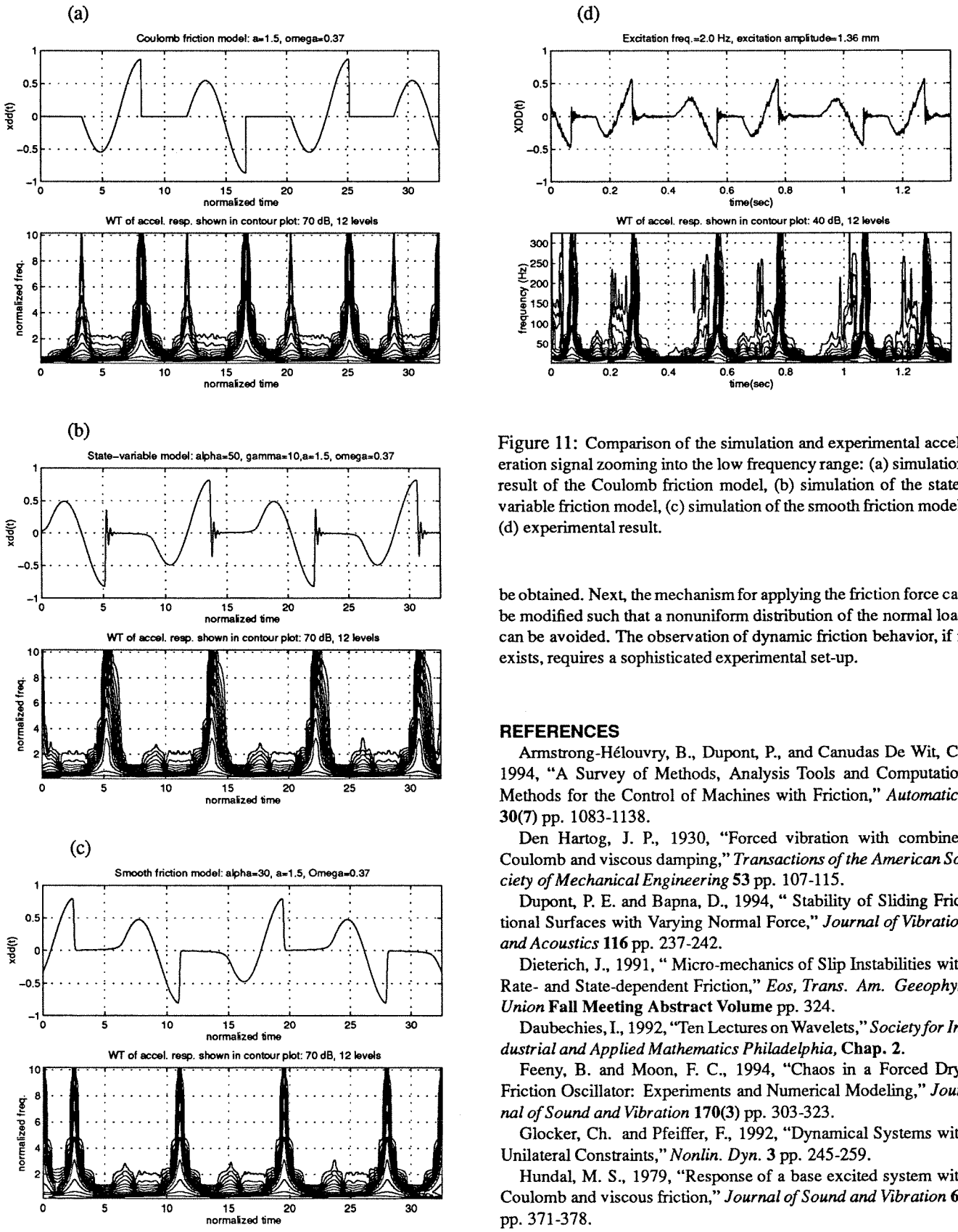

Figure 11: Comparison of the simulation and experimental acceleration signal zooming into the low frequency range: (a) simulation result of the Coulomb friction model, (b) simulation of the state-variable friction model, (c) simulation of the smooth friction model, (d) experimental result.

be obtained. Next, the mechanism for applying the friction force can be modified such that a nonuniform distribution of the normal load can be avoided. The observation of dynamic friction behavior, if it exists, requires a sophisticated experimental set-up.

REFERENCES

Armstrong-Hélouvry, B., Dupont, P., and Canudas De Wit, C., 1994, "A Survey of Methods, Analysis Tools and Computation Methods for the Control of Machines with Friction," *Automatica* **30(7)** pp. 1083-1138.

Den Hartog, J. P., 1930, "Forced vibration with combined Coulomb and viscous damping," *Transactions of the American Society of Mechanical Engineering* **53** pp. 107-115.

Dupont, P. E. and Bapna, D., 1994, " Stability of Sliding Frictional Surfaces with Varying Normal Force," *Journal of Vibration and Acoustics* **116** pp. 237-242.

Dieterich, J., 1991, " Micro-mechanics of Slip Instabilities with Rate- and State-dependent Friction," *Eos, Trans. Am. Geeophys. Union* **Fall Meeting Abstract Volume** pp. 324.

Daubechies, I., 1992, "Ten Lectures on Wavelets," *Society for Industrial and Applied Mathematics Philadelphia,* **Chap. 2.**

Feeny, B. and Moon, F. C., 1994, "Chaos in a Forced Dry-Friction Oscillator: Experiments and Numerical Modeling," *Journal of Sound and Vibration* **170(3)** pp. 303-323.

Glocker, Ch. and Pfeiffer, F., 1992, "Dynamical Systems with Unilateral Constraints," *Nonlin. Dyn.* **3** pp. 245-259.

Hundal, M. S., 1979, "Response of a base excited system with Coulomb and viscous friction," *Journal of Sound and Vibration* **64** pp. 371-378.

Morlet, J., Arens, G., Fourgeau, F., and Giard, D., 1982, "Wave

Propagation and Sampling Theory-Part I: Complex Signal and Scattering in Multi-Layered Media," *Geophysics* **47** pp. 203-221.

Propagation and Sampling Theory-Part I: Sampling Theory and Complex Waves," *Geophysics* **47** pp. 222-236.

Marui, E. and Kato, S., 1984, "Forced Vibration of a Base-Excited Single-Degree-of-Freedom System With Coulomb Friction," *Transactions of ASME, Journal of Dynamical Systems, Measurement, and Control* **106** pp. 280-285.

Meijaard, J. P., 1994, "Efficient Simulation of Systems with Discontinuities and Time-Varying Topology," *Fifth Conference on Nonlinear Vibrations, Stability, and Dynamics of Structures, Blacksburg.*

Newland, D. E., 1994, "Wavelet Analysis of Vibration, Part 1: Theory ," *Journal of Vibration and Acoustics* **116** pp. 409-416.

Newland, D. E., 1994, " Wavelet Analysis of Vibration, Part 2: Wavelet Maps," *Journal of Vibration and Acoustics* **116** pp. 417-425.

Oden, J. T. and Martins, J. A. C., 1985, "Models and Computational Methods for Dynamic Friction Phenomena," *Comput. Meth. Appl. Mech. Eng.* **52(1-3)** pp. 527-634.

Önsay and Haddow A. G., 1994, " Wavelet Transform Analysis of Transient Wave Propagation in a Dispersive Medium," *J. Accoust. Soc. Am.* **95(3)** pp. 1441-1449.

Polycarpou, A. and Soom, A., 1992, " Transitions Between Sticking and Slipping," *Friction-Induced Vibration, Chatter, Squeal, and Chaos, Proc. ASME Winter Annual Meeting, Anaheim* **DE-Vol. 49** pp. 139-148.

Pierre, C., Ferri, A., and Dowell, E. H., 1985, "Multi-Harmonic Analysis of Dry Friction Damped Systems Using an Incremental Harmonic Balance Method," *Journal of Applied Mechanics* **52(4)** pp. 958-964.

Ruina, A., 1980, "Friction Laws and Instabilities: A Quasistatic Analysis of Some Dry Frictional Behavior," *Ph. D. Dissertation, Division of Engineering, Brown University*

Shaw, S. W., 1986, "On the dynamic response of a system with dry friction," *Journal of Sound and Vibration* **108(2)** pp. 305-325.